



EXPRESSIONS FOR PREDICTING FUNDAMENTAL NATURAL FREQUENCIES OF NON-CYLINDRICAL HELICAL SPRINGS

V. YILDIRIM

Department of Mechanical Engineering, University of Çukurova, 01330 Balcalı-Adana, Turkey.

E-mail: vebil@mail.cu.edu.tr

(Received 6 July 2000, and in final form 30 July 2001)

Numerical and analytical studies are performed for the free vibration analysis of non-cylindrical (conical, barrel and hyperboloidal types) helical springs. The stiffness matrix method is used in the numerical analysis. A total of 12 degrees of freedom (six displacements and six rotations) is described for an element. The exact element stiffness matrix and the exact concentrated element inertia matrix are used in the formulation. The rotary inertia, the shear and extensional deformation effects are considered in the analysis. Comparison of the numerical results with the reported results obtained numerically and experimentally gives satisfactory values. After verification of the numerical frequencies, the non-dimensional fundamental frequencies of fixed-fixed non-cylindrical helical springs with circular section are expressed in a simple formula with a maximum absolute relative error of 5% using those numerical values for the constant helix pitch angles (5° , 10° , and 15°). These expressions restricted to the fundamental frequencies are also verified with ANSYS results.

© 2002 Elsevier Science Ltd. All rights reserved.

1. INTRODUCTION

Helical springs are commonly used in many engineering applications. There have been few theoretical and experimental studies on non-cylindrical helical springs (Figure 1) compared to those on cylindrical helical springs.

Epstein [1] worked out the free vibration of conical helical springs. He obtained the fundamental frequency of conical springs theoretically for several boundary conditions. After his pioneering work, the vibration behavior of non-cylindrical helical springs has been the subject of research in the last two decades. Nagaya *et al.* [2] studied the free vibration problem of barrel- and hyperboloidal-type helical springs both experimentally and theoretically. They used the Mayklestad method (the transfer matrix method for lumped masses) in their numerical studies. The natural frequencies for conical- barrel- and hyperboloidal-type springs were obtained in good approximations based on the stiffness matrix method by Yıldırım [3]. Yıldırım and İnce [4] studied the effects of the rotatory inertia, shear and axial deformation effects on the natural frequencies of helical springs with arbitrary shapes. Employing both the transfer matrix and the complementary functions methods, exact numerical solutions were given by Yıldırım [5]. The distributed parameter model for the free vibration analysis of non-cylindrical helical springs was used in this study. Recently, Wu and Hsu [6] calculated the load-deflection relation of the conical spring. They solved the dynamic equations by perturbation and numerical methods.

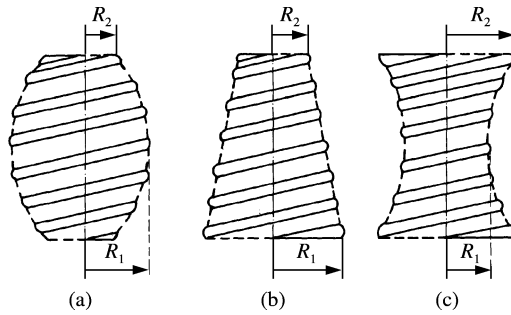


Figure 1. Types of non-cylindrical helical springs: (a) barrel; (b) conical and (c) hyperboloidal.

For non-cylindrical helical springs, there is no analytical formula to predict the natural frequencies whose values depend on many parameters such as helix pitch angle, the ratio of wire diameter to one of cylinder characteristic diameters, the ratio of minimum cylinder diameter to maximum cylinder diameter, the number of active turns, boundary conditions, type of cross-sections, etc. It is difficult to obtain derived general formulas that comprise all the effects mentioned above and their variation along the spring axis for natural frequencies of non-cylindrical helical springs. This has also not been achieved for cylindrical helical springs. At least, having some frequency expressions that can be used in some practical ranges of significant parameters will be very useful for dynamic design of such springs.

The objective of the present study is to formulate the free vibration problem of non-cylindrical helical springs in an accurate manner and obtain simple expressions for just the fundamental natural frequency of clamped-clamped springs with circular section. It was observed from Yildirim’s [7] study on cylindrical helical springs that it is possible to present natural frequencies with approximate formulae if the numerical solution is accurate. In order to achieve this, the exact non-cylindrical helical element stiffness matrix is obtained based on the transfer matrix method. The element transfer matrix is computed by numerical integration of the differential equations governing the static behavior of non-cylindrical helical springs. The exact mass of the element is used in the determination of the concentrated element inertia matrix. The subspace iteration and Jacobi’s methods are used in the solution of the large-scale eigenvalue problem [8]. This formulation yields the natural frequencies, which are very close to Yildirim’s [5] exact numerical results.

2. FORMULATION OF THE PROBLEM

Representing the state vector by \mathbf{S} , the governing equations of a helical spring can be written in matrix notation as

$$d\mathbf{S}(\phi)/d\phi = \mathbf{D}\mathbf{S}(\phi), \tag{1}$$

where ϕ is the angular co-ordinate and \mathbf{D} is the differential matrix. Derivation of equation (1) is given in the appendix. The elements of the state vector are

$$\mathbf{S}(\phi) = \{U_t, U_n, U_b, \Omega_t, \Omega_n, \Omega_b, T_t, T_n, T_b, M_t, M_n, M_b\}^T, \tag{2}$$

where $T_t, T_n,$ and T_b ($\mathbf{T} = T_t\mathbf{t} + T_n\mathbf{n} + T_b\mathbf{b}$) are the components of the internal forces on the cross-section in the \mathbf{t} -, \mathbf{n} -, and \mathbf{b} -direction (Frenet co-ordinates), respectively, and $M_t, M_n,$ and M_b ($\mathbf{M} = M_t\mathbf{t} + M_n\mathbf{n} + M_b\mathbf{b}$) are the components of the internal moments on

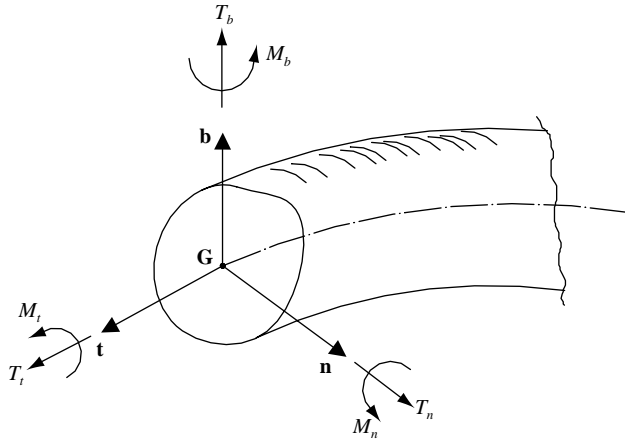


Figure 2. Stress resultants at a section of a spatial bar.

this section on the **t**-, **n**-, and **b**-direction respectively (Figure 2). U_t, U_n, U_b ($\mathbf{U} = U_t\mathbf{t} + U_n\mathbf{n} + U_b\mathbf{b}$) and $\Omega_t, \Omega_n, \Omega_b$ ($\Omega = \Omega_t\mathbf{t} + \Omega_n\mathbf{n} + \Omega_b\mathbf{b}$) are the Frenet components of the displacements and rotational vectors respectively.

The following assumptions are used in the formulation: the relationship between the forces and deformations is linear and the deformations are small. The bar is made of an elastic, homogeneous and isotropic material whose cross-sectional area is circular and uniform. Warping is neglected.

The non-zero elements of the differential matrix by these assumptions are given by Haktanır [9]:

$$\begin{aligned}
 D_{1,2} = R(\phi)/c(\phi) = -D_{2,1} = D_{4,5} = -D_{5,4} = D_{7,8} = -D_{8,7} = D_{10,11} = -D_{11,10}, \\
 D_{1,7} = c(\phi)/EA, \\
 D_{2,3} = h(\phi)/c(\phi) = -D_{3,2} = D_{5,6} = -D_{6,5} = D_{8,9} = -D_{9,8} = D_{11,12} = -D_{12,11}, \\
 D_{2,6} = c(\phi) = -D_{3,5} = D_{11,9} = -D_{12,8}, \\
 D_{2,8} = k'/c(\phi)/GA = D_{3,9}, \quad D_{4,10} = c(\phi)/2GI, \quad D_{5,11} = c(\phi)/EI = D_{6,12}, \quad (3)
 \end{aligned}$$

where k' is the shear coefficient factor, E is Young's modulus, G is the shear modulus, A is the cross-sectional area, I is the second moment of inertia and the other quantities in equations (3) are (Figures 1 and 3):

$$\begin{aligned}
 R(\phi) &= R_1 + (R_2 - R_1)(1 - \phi/\pi n)^2 \quad (\text{for both barrel and hyperboloidal springs}), \\
 R(\phi) &= R_1 + (R_2 - R_1)\phi/2\pi n \quad (\text{for conical springs}), \\
 h(\phi) &= R(\phi) \tan \alpha, \quad c(\phi) = [R^2(\phi) + h^2(\phi)]^{1/2}, \quad (4)
 \end{aligned}$$

where n is the number of active coils and α is the pitch angle of the helix. The homogeneous solution of equation (1) associated with the transfer matrix, \mathbf{F} , is [10]

$$\mathbf{S}(\phi) = \mathbf{F}(\phi)\mathbf{S}(0) \quad (5)$$

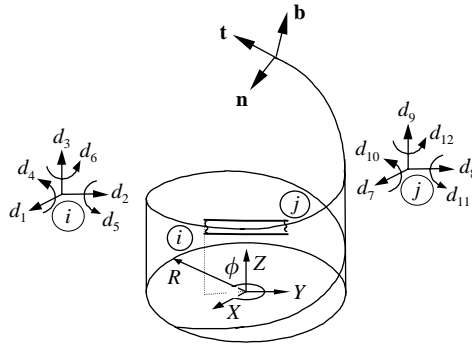


Figure 3. Degrees of freedom: t, n, b : local co-ordinates; X, Y, Z : global co-ordinates.

where $S(0)$ is the state vector at $\phi = 0$. As can be seen from equations (3), the elements of the differential matrix are not constant due to the variable curvatures along the curve. In order to obtain the transfer matrix for this case, the following differential equation must be solved 12 times for 12 different initial conditions.

$$dF^{*(m)}(\phi)/d\phi = DF^{*(m)}(\phi), \quad (m = 1, 2, \dots, 12), \tag{6}$$

where $F^{*(m)}$ denotes the solution when the m th element of the unknown vector equals 1 as its other elements are all zero. That is, the initial conditions must be satisfied as $F(0) = I$ (I is the unit matrix) [9]. These solutions compose the exact transfer matrix for non-cylindrical helical springs as

$$F = [F_{12 \times 1}^{*(1)} \quad F_{12 \times 1}^{*(2)} \quad \dots \quad F_{12 \times 1}^{*(12)}]_{12 \times 12}. \tag{7}$$

The elements of the state vector at both ends for an element can be expressed by the element end displacements, d_i and d_j , and the element end forces, p_i and p_j , as (Figure 3)

$$S(\phi_i) = \{d_1, d_2, d_3, d_4, d_5, d_6, p_1, p_2, p_3, p_4, p_5, p_6\}^T = \{d_i \quad p_i\}^T,$$

$$S(\phi_j) = \{d_7, d_8, d_9, d_{10}, d_{11}, d_{12}, p_7, p_8, p_9, p_{10}, p_{11}, p_{12}\}^T = \{d_j \quad p_j\}^T. \tag{8}$$

Using the above definitions, equation (5) can be rearranged for an element as

$$S(\phi_j) = F(\phi_j - \phi_i)S(\phi_i). \tag{9}$$

The element transfer matrix can be expressed in global co-ordinates as (Figure 3)

$$F_{XYZ}(\phi_j - \phi_i) = T^{-1}(\phi_j)F_{mb}(\phi_j - \phi_i)T(\phi_i), \tag{10}$$

where

$$T = \begin{bmatrix} \mathbf{B} & 0 & 0 & 0 \\ 0 & \mathbf{B} & 0 & 0 \\ 0 & 0 & \mathbf{B} & 0 \\ 0 & 0 & 0 & \mathbf{B} \end{bmatrix} \tag{11}$$

and

$$\mathbf{B} = \begin{bmatrix} -[R(\phi)/c(\phi)] \sin \phi & [R(\phi)/c(\phi)] \cos \phi & h(\phi)/c(\phi) \\ -\cos \phi & -\sin \phi & 0 \\ [h(\phi)/c(\phi)] \sin \phi & -[h(\phi)/c(\phi)] \cos \phi & R(\phi)/c(\phi) \end{bmatrix}. \quad (12)$$

The element stiffness equation is given by

$$\mathbf{p} = \mathbf{k}\mathbf{d}, \quad (13a)$$

or

$$\{\mathbf{p}_i \ \mathbf{p}_j\}^T = \mathbf{k}\{\mathbf{d}_i \ \mathbf{d}_j\}^T, \quad (13b)$$

where \mathbf{k} is the element stiffness matrix. The elements of \mathbf{k} are obtained by solving equation (9) 12 times for 12 boundary conditions which are determined by considering the definition of the element transfer matrix [3, 9]. It may be noted that the element end forces at ϕ_i are obtained for positive sections in the transfer matrix method.

The solution of the free vibration problem is given by

$$(\mathbf{K} - \omega^2\mathbf{M})\mathbf{a} = 0, \quad (14)$$

where \mathbf{K} is the global stiffness matrix, \mathbf{M} is the global inertia matrix, \mathbf{a} is the amplitude vector and ω (rad/s) is the angular frequency.

Assuming that the total element mass is equally transferred at the two ends, the non-zero terms of the concentrated element mass matrix \mathbf{m} , which are the same in all the co-ordinate systems, are obtained as

$$m_{1,1} = m_{2,2} = m_{3,3} = m_{7,7} = m_{8,8} = m_{9,9} = \rho AL_{element}/2, \\ m_{4,4} = m_{10,10} = \rho IL_{element}, \quad m_{5,5} = m_{6,6} = m_{11,11} = m_{12,12} = \rho IL_{element}/2, \quad (15)$$

where the total length of the conical element is

$$L_{element} = \frac{1}{\cos \alpha} \int_{\phi_i}^{\phi_j} R(\phi) d\phi = \frac{1}{4 \cos \alpha} \left\{ \frac{4\phi_j R_1 \pi n + (R_2 - R_1)\phi_j^2 - 4R_1 \phi_i \pi n + (R_1 - R_2)\phi_i^2}{\pi n} \right\} \quad (16)$$

and that of the barrel and hyperboloidal elements is

$$L_{element} = \frac{1}{\cos \alpha} \int_{\phi_i}^{\phi_j} R(\phi) d\phi = \frac{1}{\cos \alpha} \left\{ R_2(\phi_j - \phi_i) + \frac{R_2}{3\pi^2 n^2} (\phi_j^3 - \phi_i^3) \right. \\ \left. + \frac{R_1}{3\pi^2 n^2} (\phi_i^3 - \phi_j^3) + \frac{R_2}{\pi n} (\phi_i^2 - \phi_j^2) + \frac{R_1}{\pi n} (\phi_j^2 - \phi_i^2) \right\}. \quad (17)$$

For simplicity, a lumped mass model is used in this study instead of a distributed mass model. As can be seen from equation (15), the lumped mass matrix comprises the rotatory

inertia terms. Since the exact mass of the element derived by equations (15)–(17) and also the exact element stiffness matrix are used together, the present formulation gives satisfactory results.

3. APPLICATIONS

To compare the accuracy of the present results with the reported values, conical-, barrel- and hyperboloidal-type springs having the same maximum cylinder diameter has been examined and the results are presented in Table 1 in which natural frequencies given by Nagaya *et al.* [2] in graphical forms were determined approximately. The shear and rotary inertia effects were neglected in their study and also the transfer matrix method is used with the discrete parameter model [2]. The free vibration problem was formulated by Yıldırım [3] based on the stiffness matrix method. The exact cylindrical element stiffness matrix and the consistent element inertia matrix for straight beams are used in the analysis [3]. A good agreement is observed with the reported results. The present numerical frequencies coincide with the exact results [5].

Helical springs exhibit some very close frequencies. In some cases, it is difficult to obtain those frequencies as can be seen in Table 2. Nagaya *et al.* [2] skipped the natural frequencies associated with the third and fourth modes of barrel spring for all R_{min}/R_{max} ratios.

To express the fundamental frequencies in the analytical form, a number of examples have been solved and presented in the non-dimensional graphical form for all types of helices with circular section. The non-dimensional frequency is determined by

$$\varpi = \sqrt{(\rho AR_{max}^4/EI)}\omega. \quad (18)$$

Variation of the numerical fundamental frequencies with the helix angle, R_{min}/R_{max} ratios, and the number of turns is presented in Figure 4 for $D_{max}/d = 4$.

TABLE 1

Comparison of the present fundamental numerical frequencies (in Hertz) with the existing results

		Fundamental natural frequencies (Hz)			
		R_{min}/R_{max}			
		0.2	0.4	0.6	0.8
Hyperboloidal	Yıldırım [3] [†]	121.77	92.83	71.68	55.91
	Present [‡]	121.39	92.73	71.65	55.90
	Nagaya <i>et al.</i> [2] [§]	71.0	64.0	59.0	52.0
	Nagaya <i>et al.</i> [2] [§]	–	66.0	60.0	52.0
Barrel	Yıldırım [5] ^{exact}	71.86	65.53	59.62	52.11
	Yıldırım [3] [†]	72.96	65.53	60.37	52.16
	Present [‡]	71.85	65.53	59.62	52.11
Conical	Yıldırım [3] [†]	110.56	88.30	68.90	54.53
	Present [‡]	108.18	87.39	68.52	54.39

[†]100 elements [‡]theoretical (78 elements), [§]experimental.

{ $E = 2.1 \times 10^{11}$ N/m², $\nu = 0.3$ (the Poisson ratio), $\rho = 7850$ kg/m³ (the mass density), $\alpha = 4.8^\circ$, $n = 6.5$, fixed–fixed, $R_{max} = D_{max}/2 = 25$ mm (radius of the maximum cylinder), $k' = 1.1$, $d = 2$ mm (diameter of the section)}.

TABLE 2

The first six natural frequencies (in Hertz) of barrel spring ($R_1/R_2 = 0.4$)

	1	2	3	4	5	6
Nagaya <i>et al.</i> [2] [†]	64.0	71.0	–	–	129.0	134.0
Nagaya <i>et al.</i> [2] [‡]	66.0	72.0	–	–	129.0	136.0
ANSYS [§]	67.07	73.46	88.50	88.57	133.04	138.64
Yıldırım [5] ^{exact}	65.53	71.52	86.94	87.01	129.60	–
Present (numerical) [§]	65.53	71.51	86.93	86.99	129.58	135.00

[†]theoretical (78 elements), [‡]experimental, [§]100 elements.

Material and helix geometrical properties are the same as in Table 1.

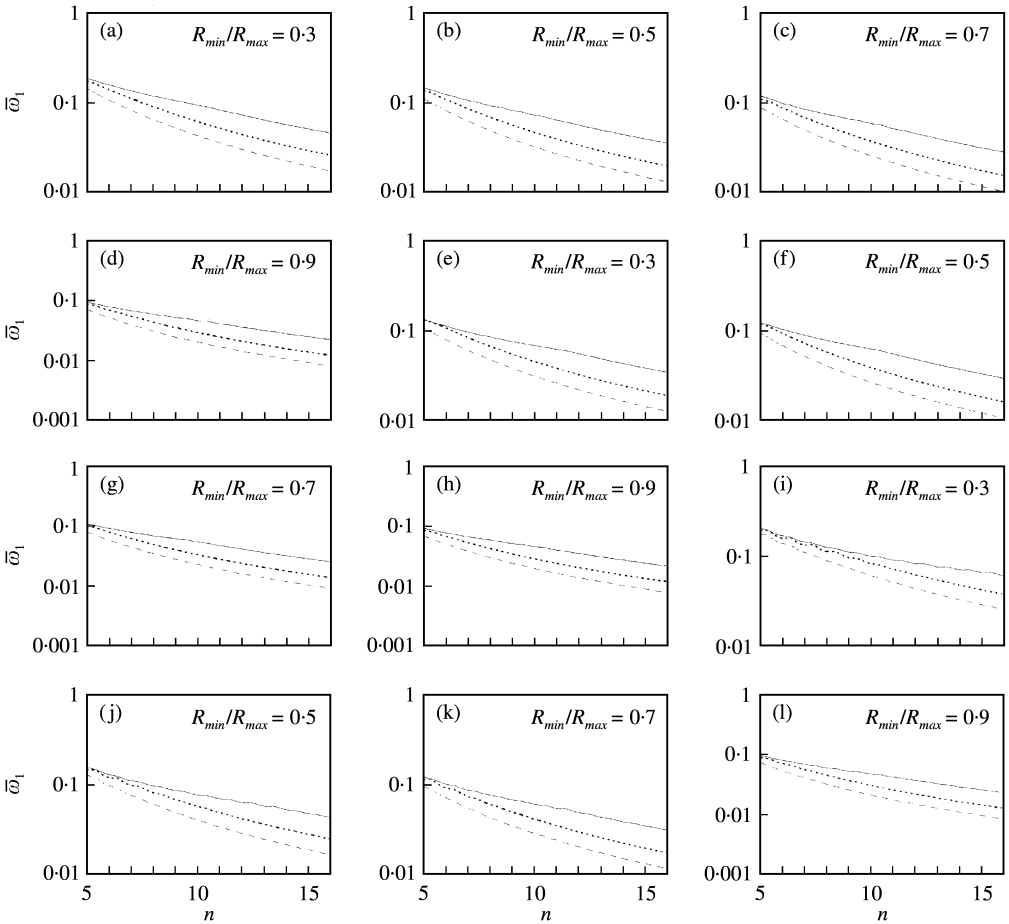


Figure 4. Variation of dimensionless fundamental frequencies with helix pitch angle, α , R_{min}/R_{max} ratios and number of active turns, n , for $D_{max}/d = 4$. Figures (a)–(d) refer to conical springs, (e)–(h) Barrel springs and (i)–(l) hyperboloidal springs. Key for helix pitch angle, α : —, 5°; ---, 10°; ···, 15°.

4. RESULTS

The following simple expression is obtained for the fundamental natural frequencies of non-cylindrical helical springs (the Poisson ratio = $\nu = 0.3$).

$$\omega_1^{expression} = [a \ln(n - 4.8/0.2) + b](1 + CF), \tag{19}$$

where the correlation factor is (the argument of cosine is in radians)

$$CF = A/100 \cos[2\pi/T(n - 4.8/0.2) + 2\pi(1 - F/T)]. \tag{20}$$

The constants a and b in equation (19) are presented in Tables 3–5 for the values of $D_{max}/d = 4, 6, 8, 10, 12$, $\alpha = 5^\circ, 10^\circ, 15^\circ$, and $R_{min}/R_{max} = 0.3, 0.5, 0.7, 0.9$. The values of constants A, T , and F in equation (20) are given in Table 6 with respect to the values of α and R_{min}/R_{max} . These values are valid for $D_{max}/d = 4, 6, 8, 10$, and 12 . The valid intervals of the number of active coils for Table 6 and the maximum absolute relative errors in these intervals are presented in Table 7. The maximum absolute relative error is determined as

$$\text{Relative error} = \left| \frac{\varpi_1^{expression} - \varpi_1^{numeric}}{\varpi_1^{numeric}} \right| \times 100. \tag{21}$$

A comparison of the numerical and analytical results obtained in this study with the ANSYS results is presented in Table 8. The absolute relative errors are given in parentheses with respect to the present numerical frequencies. It is observed from Table 8 that the present formula gives acceptable results for engineering applications. If the ratio R_{min}/R_{max} decreases while $D_{max}/d, n$ and α are still constant, the relative errors of ANSYS' results increase. The maximum absolute relative error of analytical frequencies cannot be more than 5% for a given interval of the number of coils presented in Table 7.

TABLE 3

The constants a and b in equation (19) for hyperboloidal springs

D_{max}/d	R_{min}/R_{max}	$\alpha = 5^\circ$		$\alpha = 10^\circ$		$\alpha = 15^\circ$	
		a	b	a	b	a	b
4	0.3	-0.0427	0.2379	-0.0496	0.2428	-0.0466	0.2135
	0.5	-0.0335	0.1842	-0.0390	0.1839	-0.0337	0.1512
	0.7	-0.0269	0.1451	-0.0304	0.1404	-0.0248	0.1103
	0.9	-0.0217	0.1153	-0.0237	0.1084	-0.0187	0.0829
6	0.3	-0.0434	0.2417	-0.0504	0.2463	-0.0471	0.2155
	0.5	-0.0341	0.1869	-0.0395	0.1860	-0.0340	0.1523
	0.7	-0.0273	0.1470	-0.0307	0.1416	-0.0250	0.1109
	0.9	-0.0220	0.1165	-0.0239	0.1092	-0.0188	0.0833
8	0.3	-0.0437	0.2431	-0.0507	0.2475	-0.0473	0.2163
	0.5	-0.0343	0.1879	-0.0397	0.1868	-0.0341	0.1527
	0.7	-0.0274	0.1477	-0.0308	0.1421	-0.0250	0.1111
	0.9	-0.0221	0.1170	-0.0240	0.1094	-0.0189	0.0834
10	0.3	-0.0438	0.2437	-0.0509	0.2481	-0.0474	0.2166
	0.5	-0.0344	0.1884	-0.0398	0.1872	-0.0341	0.1529
	0.7	-0.0275	0.1480	-0.0309	0.1423	-0.0250	0.1112
	0.9	-0.0221	0.1172	-0.0240	0.1095	-0.0189	0.0835
12	0.3	-0.0439	0.2441	-0.0509	0.2484	-0.0474	0.2168
	0.5	-0.0344	0.1886	-0.0398	0.1874	-0.0342	0.1530
	0.7	-0.0276	0.1481	-0.0309	0.1424	-0.0251	0.1120
	0.9	-0.0221	0.1173	-0.0240	0.1096	-0.0189	0.0835

TABLE 4

The constants a and b in equation (19) for conical springs

D_{max}/d	R_{min}/R_{max}	$\alpha = 5^\circ$		$\alpha = 10^\circ$		$\alpha = 15^\circ$	
		<i>a</i>	<i>b</i>	<i>a</i>	<i>b</i>	<i>a</i>	<i>b</i>
4	0.3	-0.0422	0.2249	-0.0453	0.2093	-0.0369	0.1645
	0.5	-0.0338	0.1785	-0.0361	0.1653	-0.0286	0.1270
	0.7	-0.0268	0.1415	-0.0288	0.1314	-0.0226	0.1001
	0.9	-0.0216	0.1140	-0.0233	0.1061	-0.0182	0.0805
6	0.3	-0.0430	0.2291	-0.0459	0.2118	-0.0373	0.1657
	0.5	-0.0345	0.1817	-0.0366	0.1671	-0.0289	0.1278
	0.7	-0.0272	0.1434	-0.0291	0.1325	-0.0228	0.1006
	0.9	-0.0218	0.1152	-0.0235	0.1068	-0.0183	0.0808
8	0.3	-0.0433	0.2304	-0.0461	0.2127	-0.0374	0.1662
	0.5	-0.0347	0.1829	-0.0367	0.1677	-0.0289	0.1280
	0.7	-0.0274	0.1441	-0.0292	0.1329	-0.0228	0.1007
	0.9	-0.0219	0.1157	-0.0236	0.1071	-0.0183	0.0810
10	0.3	-0.0435	0.2311	-0.0462	0.2131	-0.0374	0.1664
	0.5	-0.0348	0.1834	-0.0368	0.1680	-0.0290	0.1282
	0.7	-0.0274	0.1445	-0.0293	0.1331	-0.0228	0.1008
	0.9	-0.0220	0.1159	-0.0236	0.1072	-0.0183	0.0810
12	0.3	-0.0435	0.2314	-0.0463	0.2133	-0.0375	0.1665
	0.5	-0.0349	0.1837	-0.0369	0.1682	-0.0290	0.1282
	0.7	-0.0275	0.1446	-0.0293	0.1332	-0.0228	0.1009
	0.9	-0.0220	0.1160	-0.0236	0.1072	-0.0184	0.0811

TABLE 5

The constants a and b in equation (19) for barrel springs

D_{max}/d	R_{min}/R_{max}	$\alpha = 5^\circ$		$\alpha = 10^\circ$		$\alpha = 15^\circ$	
		<i>a</i>	<i>b</i>	<i>a</i>	<i>b</i>	<i>a</i>	<i>b</i>
4	0.3	-0.0294	0.1599	-0.0350	0.1600	-0.0278	0.1230
	0.5	-0.0278	0.1476	-0.0311	0.1408	-0.0238	0.1052
	0.7	-0.0252	0.1322	-0.0268	0.1211	-0.0205	0.0905
	0.9	-0.0213	0.1123	-0.0228	0.1037	-0.0177	0.0781
6	0.3	-0.0295	0.1606	-0.0352	0.1612	-0.0280	0.1237
	0.5	-0.0279	0.1484	-0.0314	0.1420	-0.0240	0.1058
	0.7	-0.0255	0.1337	-0.0270	0.1221	-0.0206	0.0909
	0.9	-0.0216	0.1135	-0.0230	0.1044	-0.0178	0.0785
8	0.3	-0.0295	0.1609	-0.0353	0.1615	-0.0281	0.1240
	0.5	-0.0279	0.1486	-0.0315	0.1424	-0.0240	0.1060
	0.7	-0.0256	0.1342	-0.0271	0.1224	-0.0207	0.0911
	0.9	-0.0217	0.1139	-0.0231	0.1046	-0.0178	0.0786
10	0.3	-0.0295	0.1610	-0.0354	0.1617	-0.0281	0.1241
	0.5	-0.0279	0.1487	-0.0315	0.1425	-0.0241	0.1061
	0.7	-0.0257	0.1344	-0.0271	0.1226	-0.0207	0.0911
	0.9	-0.0217	0.1141	-0.0231	0.1047	-0.0178	0.0786
12	0.3	-0.0295	0.1610	-0.0354	0.1618	-0.0281	0.1242
	0.5	-0.0279	0.1488	-0.0316	0.1426	-0.0241	0.1061
	0.7	-0.0257	0.1346	-0.0272	0.1226	-0.0207	0.0912
	0.9	-0.0218	0.1142	-0.0231	0.1048	-0.0178	0.0786

TABLE 6

Values of constants $A, T, \text{ and } F$ in equation (20)

α ($^\circ$)	R_{min}/R_{max}	Hyperboloidal			Conical			Barrel		
		A	T	F	A	T	F	A	T	F
5	0.3	7.1	76.0	11.0	11.5	62.0	21.5	11.2	60.5	21.5
	0.5	9.1	79.0	16.0	11.5	62.0	21.5	11.2	60.5	21.5
	0.7	10.6	78.0	13.0	11.5	62.0	21.5	11.2	60.5	21.5
	0.9	11.6	78.0	13.0	11.5	62.0	21.5	11.2	60.5	21.5
10	0.3	11.0	79.0	11.6	10.5	57.0	11.8	9.1	58.0	11.4
	0.5	9.5	79.0	11.6	10.5	57.0	11.8	9.1	58.0	11.4
	0.7	11.0	77.0	1.6	10.5	57.0	11.8	9.1	58.0	11.4
	0.9	11.0	77.0	1.6	10.5	57.0	11.8	9.1	58.0	11.4
15	0.3	8.3	75.0	2.1	6.3	50.0	11.1	6.3	48.0	11.1
	0.5	7.3	69.0	0.8	6.3	50.0	11.1	6.3	48.0	11.1
	0.7	10.3	66.5	0.0	6.3	50.0	11.1	6.3	48.0	11.1
	0.9	10.3	63.0	0.0	6.3	50.0	11.1	6.3	48.0	11.1

TABLE 7

The valid interval of n for Table 6 and maximum absolute relative errors in the interval

α ($^\circ$)	R_{min}/R_{max}	Hyperboloidal		Conical		Barrel	
		Interval for n	Maximum rel. error	Interval for n	Maximum rel. error	Interval for n	Maximum rel. error
5	0.3	5.8–16.0	4.8	5.2–15.2	5.0	5.2–15.0	5.0
	0.5	5.6–15.6	4.9	5.2–15.2	5.0	5.2–14.6	4.5
	0.7	6.2–15.2	4.7	5.2–15.0	4.9	5.2–14.6	5.0
	0.9	6.2–15.2	4.9	5.2–15.0	4.9	5.2–14.8	4.9
10	0.3	6.2–16.0	4.9	5.6–15.4	4.8	5.6–16.0	5.0
	0.5	6.0–16.0	4.9	5.4–16.0	4.7	5.4–16.0	4.7
	0.7	6.0–16.0	4.7	5.4–16.0	4.9	5.4–16.0	5.0
	0.9	6.0–16.0	4.2	5.4–16.0	5.0	5.4–16.0	4.5
15	0.3	6.0–16.0	4.2	5.4–15.8	3.9	5.4–15.6	4.5
	0.5	5.4–16.0	4.2	5.4–15.6	4.6	5.4–15.4	4.6
	0.7	5.8–16.0	5.0	5.4–15.4	4.7	5.4–15.4	4.6
	0.9	5.6–15.8	5.0	5.4–15.4	5.0	5.4–15.6	4.6

5. CONCLUSIONS

Considering rotary inertia, shear deformation and axial effects, the free vibration analysis of non-cylindrical helical springs has been studied numerically by the stiffness method. The numerical procedure presented in this paper offers accurate natural frequencies associated with higher modes. The present numerical frequencies have compared well with other published results obtained theoretically and experimentally. Using these numerical results, an analytical study which is restricted to the fundamental frequencies has been performed for practical use in design. A simple analytical expression has been presented with

TABLE 8

Comparison of the present numerical and expressional fundamental frequencies (in Hertz) with the ANSYS results

		R_{min}/R_{max}			
		$\alpha = 5^\circ$		$\alpha = 15^\circ$	
		0.5	0.9	0.5	0.9
Hyperboloidal	Present (Numerical)	245.91	150.11	127.08	66.13
	ANSYS	265.72 (8.1%)	160.74 (7.1%)	131.07 (3.1%)	68.11 (3.0%)
	Present [equation (19)]	257.03 (4.5%)	151.39 (0.9%)	125.94 (-0.9%)	63.31 (-4.3%)
Conical	Present (numerical)	234.03	147.96	102.00	63.92
	ANSYS	250.00 (6.8%)	158.01 (6.8%)	105.95 (3.9%)	65.91 (3.1%)
	Present [equation (19)]	244.57 (4.5%)	154.46 (4.4%)	104.75 (2.7%)	66.41 (3.9%)
Barrel	Present (numerical)	196.49	145.36	83.22	61.81
	ANSYS	212.04 (7.9%)	154.69 (6.4%)	85.70 (3.0%)	63.65 (3.0%)
	Present [equation (19)]	201.29 (2.4%)	151.59 (4.3%)	85.69 (3.0%)	63.72 (3.1%)

$$\{E = 2.1 \times 10^{11} \text{ N/m}^2, \nu = 0.3, \rho = 7850 \text{ kg/m}^3, R_{max} = 13 \text{ mm}, d = 2.6 \text{ mm}, D_{max}/d = 10, n = 10\}$$

a maximum absolute relative error of 5%. The analytical expression works in a wide range of the vibrational parameters, which have been chosen as the D_{max}/d ratios (4, 6, 8, 10, 12), R_{min}/R_{max} ratios (0.3, 0.5, 0.7, 0.9), the number of active turns ($n = 5.2$ –16) and the helix pitch angles ($\alpha = 5^\circ, 10^\circ, 15^\circ$). The soundness of the analytical expressions are justified with the ANSYS results.

Since there is no formula to be used for predicting the natural frequencies of non-cylindrical helical springs in the literature, the frequency expressions obtained in this study can be a valuable tool for spring designers.

ACKNOWLEDGMENT

This work was supported by the Research Foundation of Çukurova University (FBE.98.YL.59).

REFERENCES

1. I. EPSTEIN 1947 *Journal of Applied Physics* **18**, 368–374. The motion of a conical coil springs.
2. K. NAGAYA, S. TAKEDA and Y. NAKATA 1986 *International Journal for Numerical Methods in Engineering* **23**, 1081–1099. Free vibration of coil spring of arbitrary shape.
3. V. YILDIRIM 1998 *Journal of Applied Mechanics* **65**, 157–163. A parametric study on the free vibration of non-cylindrical helical springs.
4. V. YILDIRIM and N. INCE 1997 *Journal of Sound and Vibration* **204**, 311–329. Natural frequencies of helical springs of arbitrary shape.
5. V. YILDIRIM 1997 *Communications in Numerical Methods in Engineering* **13**, 487–494. Free vibration analysis of non-cylindrical coil springs by combined use of the transfer matrix and the complementary functions methods.

6. M. H. WU and W. Y. HSU 1998 *Journal of Sound and Vibration* **214**, 17–28. Modelling the static and dynamic behavior of a conical spring by considering the coil close and damping effects.
7. V. YILDIRIM 1999 *International Journal of Mechanical Sciences* **41**, 919–939. An efficient numerical method for predicting the natural frequencies of cylindrical helical springs.
8. K. J. BATHE and E. L. WILSON 1976 *Numerical Methods in Finite Element Analysis*. Englewood Cliffs, NJ: Prentice-Hall.
9. V. HAKTANIR 1995 *International Journal for Numerical Methods in Engineering* **38**, 1031–1056. The complementary functions method for the element stiffness matrix of arbitrary spatial bars of helicoidal axes.
10. E. C. PESTEL and F. A. LECKIE 1963 *Matrix Methods in Elastomechanics*. New York: McGraw-Hill.

APPENDIX A: DERIVATION OF EQUATIONS FOR STATICAL ANALYSIS OF NON-CYLINDRICAL HELICAL BARS

For the space rod analysis, it is suitable to use Frenet co-ordinates, $(\mathbf{t}, \mathbf{n}, \mathbf{b})$, defined by the derivatives of the position vector, \mathbf{r} , to the position as in equation (A.1).

$$\mathbf{t} = d\mathbf{r}/ds, \quad \mathbf{n} = (d\mathbf{t}/ds)/(dt/ds), \quad \mathbf{b} = \mathbf{t} \times \mathbf{n}, \quad (\text{A.1})$$

where \mathbf{t} , \mathbf{n} , and \mathbf{b} denote the tangential, normal and binormal unit vectors respectively (Figure 1) and ds is the infinitesimal arc length. The relationship among the Frenet unit vectors is given as

$$d\mathbf{t}/ds = \chi\mathbf{n}, \quad d\mathbf{n}/ds = \tau\mathbf{b} - \chi\mathbf{t}, \quad d\mathbf{b}/ds = -\tau\mathbf{n}, \quad (\text{A.2})$$

where χ and τ represent the curvature and tortuosity of a curve in space. These quantities are functions of parameter s (or ϕ) for non-cylindrical helical springs. The equations of compatibility assuming small displacements and rotations are expressed as

$$d\boldsymbol{\Omega}/ds = \boldsymbol{\omega}, \quad d\mathbf{U}/ds + \mathbf{t} \times \boldsymbol{\Omega} = \boldsymbol{\gamma}, \quad (\text{A.3})$$

where $\boldsymbol{\gamma}$ and $\boldsymbol{\omega}$ are the displacement angular rotation vectors per unit length of the bar. Assuming that (1) the centroid and the shear center of the cross-section coincide, (2) the principal axes of inertia and (\mathbf{n}, \mathbf{b}) match, (3) the warping of the cross-section due to the torsion is negligible, and (4) the bar material is elastic and isotropic, the components of the non-isothermal resultant constitutive equations are written as

$$\gamma_i = A_{ij}^{-1} T_j; \quad \omega_i = C_{ij}^{-1} M_j \quad (i, j = 1, 2, 3). \quad (\text{A.4})$$

Here

$$\mathbf{A}^{-1} = \begin{bmatrix} 1/EA & 0 & 0 \\ 0 & k'/GA & 0 \\ 0 & 0 & k'/GA \end{bmatrix}; \quad \mathbf{C}^{-1} = \begin{bmatrix} 1/GJ & 0 & 0 \\ 0 & 1/EI_n & 0 \\ 0 & 0 & 1/EI_b \end{bmatrix}, \quad (\text{A.5})$$

where A is the undeformed cross-sectional area of the cross-section. I_n and I_b represent the inertia moments about the normal and binormal axes respectively. E and G represent Young's modulus and shear modulus respectively. k' is the shear correction factor and J is the torsional inertia moment of the cross-section. For the circular cross-section

$$I_n = I_b = I, \quad J = 2I. \quad (\text{A.6})$$

By inserting the constitutive equations (A.4) into the equations of compatibility, (A.3),

$$d\mathbf{U}/ds = \mathbf{A}^{-1}\mathbf{T} + \boldsymbol{\Omega} \times \mathbf{t}, \quad d\boldsymbol{\Omega}/ds = \mathbf{C}^{-1}\mathbf{M}, \quad (\text{A.7})$$

relative shear and twist vectors can be eliminated. The equations of equilibrium are

$$d\mathbf{T}/ds = 0, \quad d\mathbf{M}/ds + \mathbf{t} \times \mathbf{T} = 0, \quad (\text{A.8})$$

where distributed external forces and moments acting on a unit length of the bar are neglected to obtain the element stiffness matrix. Equation (A.7) reduced in this manner and equation (A.8) can be written in scalar forms for spatial bars with curved axes as

$$\begin{aligned} dU_t/ds &= \chi(\phi)U_n + T_t/A_{11}, & dU_n/ds &= -\chi(\phi)U_t + \tau(\phi)U_b + \Omega_b + T_n/A_{22}, \\ dU_b/ds &= -\tau(\phi)U_n - \Omega_n + T_b/A_{33}, & d\Omega_t/ds &= \chi(\phi)\Omega_n + M_t/C_{11}, \\ d\Omega_n/ds &= -\chi(\phi)\Omega_t + \tau(\phi)\Omega_b + M_n/C_{22}, & d\Omega_b/ds &= -\tau(\phi)\Omega_n + M_b/C_{33}, \\ dT_t/ds &= \chi(\phi)T_n, & dT_n/ds &= \tau(\phi)T_b - \chi(\phi)T_t, & dT_b/ds &= -\tau(\phi)T_n, \\ dM_t/ds &= \chi(\phi)M_n, \\ dM_n/ds &= \tau(\phi)M_b - \chi(\phi)M_t + T_b, & dM_b/ds &= -\tau(\phi)M_n - T_n. \end{aligned} \quad (\text{A.9})$$

These make up a set of 12 simultaneous differential equations with variable coefficients each one involving first degree derivatives with respect to position. The infinitesimal length of the non-cylindrical helix may be rewritten as

$$ds = c(\phi)d\phi. \quad (\text{A.10})$$

The curvature and tortuosity of the wire wrapped helically on the non-cylindrical surface can be written in the form [see equation (4) in the main text]

$$\chi(\phi) = R(\phi)/c^2(\phi), \quad \tau(\phi) = h(\phi)/c^2(\phi). \quad (\text{A.11})$$

Finally, considering equation (2) in the main text and equations (A.9–A.11), the statical equations will generalize to

$$d\mathbf{S}(\phi)/d\phi = \mathbf{DS}(\phi). \quad (\text{A.12})$$